DØnote 5126-CONF

Search for the associated production of charginos and neutralinos in the like sign dimuon channel

The DØ Collaboration
URL http://www-d0.fnal.gov
(Dated: June 30, 2006)

A search for the associated production of charginos and neutralinos has been performed in $p\bar{p}$ collisions recorded with the DØ detector at a center of mass energy of 1.96 TeV at the Tevatron collider. The final state with two like sign muons and missing transverse energy is under consideration. A dataset corresponding to an integrated luminosity of roughly 1 fb^{-1} has been analyzed. For mSUGRA scenarios with enhanced leptonic branching fractions, a $\widetilde{\chi}_1^{\pm}$ mass limit beyond the reach of LEP searches has been set.

Preliminary Results for Summer 2006 Conferences

I. INTRODUCTION

Supersymmetry is a proposed symmetry relating bosonic and fermionic states [1]. The minimal supersymmetric extension of the standard model, the MSSM [2], implies the existence of a new spectrum of particles where every particle of the standard model gets a supersymmetric partner (so called sparticles). The sparticle mass spectrum is unknown, and it is possible that only some of the lighest sparticles would be observable at the Tevatron. In the mSUGRA supersymmetry breaking scenario [3], neutralinos and charginos, which are a mixing of the superpartners of the electroweak gauge bosons and the Higgs bosons, are considered promising candidates for a discovery at the Tevatron. In R-parity conserving theories [4], sparticles are pair produced from $p\bar{p}$ collisions and the lightest supersymmetric particle (LSP), which is stable, escapes detection leading to a significant amount of missing transverse energy. The associated production of the lightest chargino, $\widetilde{\chi}_1^{\pm}$, and the next to lightest neutralino, $\widetilde{\chi}_2^0$, decaying into three leptons and missing transverse energy leads to a clean signature with low standard model background. This final state is referred as the trilepton channel. The associated production of the $\widetilde{\chi}_1^{\pm}$ and $\widetilde{\chi}_2^0$ takes place via an off-shell W boson in the s channel or a squark exchange in the t channel. The corresponding graphs are presented in Figure 1. As illustrated in Figure 2, $\widetilde{\chi}_1^{\pm}$ and $\widetilde{\chi}_2^0$ decay through virtual gauge bosons or sleptons into leptons accompanied by particles escaping detection (neutrino or LSP).

FIG. 1: Graphs for $\widetilde{\chi}_1^{\pm}/\widetilde{\chi}_2^0$ pair production.

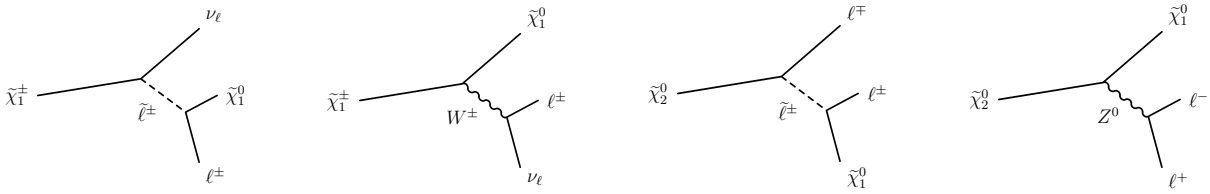

FIG. 2: Graphs for $\widetilde{\chi}_1^{\pm}$ and $\widetilde{\chi}_2^0$ decays in leptonic final states.

The leptonic decays of $\widetilde{\chi}_1^{\pm}$ and $\widetilde{\chi}_2^0$ lead to a final state with three leptons and missing transverse energy. For some sets of parameters in the mSUGRA parameter space, the third lepton may be very soft, especially if the mass difference between $\widetilde{\chi}_2^0$ and $\widetilde{\ell}_R$ is small. Distributions of the transverse momentum for both the three leptons and like sign pair are displayed in Figure 3.

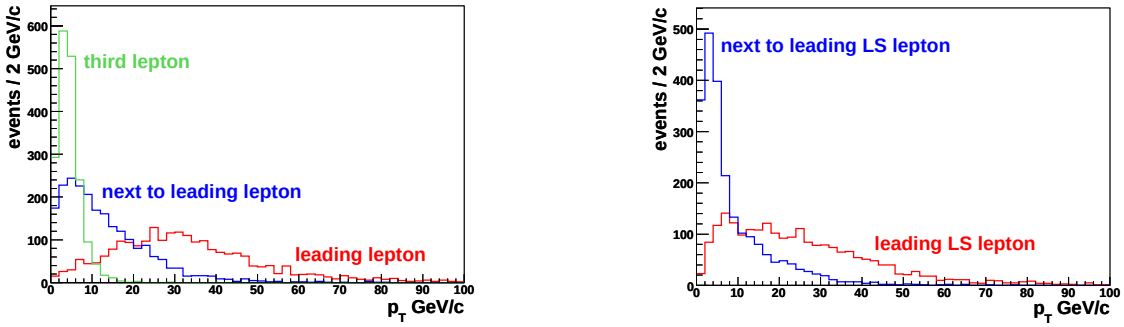

FIG. 3: Generator level distributions of the tranverse momentum (p_T) for the leptons coming from the process $\widetilde{\chi}_1^{\pm}\widetilde{\chi}_2^0 \rightarrow 3\ell$ considering the three leptons (left) and only the like sign pair (right). Leptons are sorted with respect to their p_T. The mSUGRA parameters are $m_0 = 72$ GeV/c^2, $m_{1/2} = 175$ GeV/c^2, $\tan\beta = 3$, $A_0 = 0$ GeV/c^2 and $\mu > 0$ corresponding to the following masses: $m_{\widetilde{\ell}_R} = 104.4$ GeV/c^2, $m_{\widetilde{\chi}_2^0} = 112.4$ GeV/c^2.

Previous searches at DØ have set limits on the associated production of $\widetilde{\chi}_1^{\pm}\widetilde{\chi}_2^0$ [5]. Since most of the selections are relying on the reconstruction of all three leptons, efficiencies are very low for points in the mSUGRA parameter space leading to small mass difference between $\widetilde{\ell}_R$ and $\widetilde{\chi}_2^0$. Therefore, a like sign leptons signature has been developed to deal with such a topology. Search for supersymmetry in the like sign dimuon channel is presented hereafter.

II. DATA SAMPLES

The selection is based on data collected from April 2002 up to February 2006 by the DØ detector at the Fermilab Tevatron collider at a center of mass energy of 1.96 TeV and corresponds to an integrated luminosity of 0.9 fb^{-1}. All simulated signal and standard model processes have been generated with `PYTHIA 6.323` [6] using a `CTEQ6L1` parton distribution function and processed through the full detector simulation. The masses and decays of sparticles are computed with `Spheno 2.2.3` [7] and interfaced to `PYTHIA` using `SUSY Les Houches Accords` [8]. Masses of $\widetilde{\chi}_1^{\pm}$ beyond LEP limit of 103.5 GeV/c^2 [9] are under consideration. The signal points used to optimize the selection correspond to a choice of $m_{\widetilde{\ell}_R} \lesssim m_{\widetilde{\chi}_2^0}$. The two body decay $\widetilde{\chi}_2^0 \to \widetilde{\ell}_R^{\pm}\ell^{\mp}$ is then enhanced, leading to final states with a very soft third lepton. The other mSUGRA parameters are set to the following values: $\tan\beta = 3$, $A_0 = 0$ GeV/c^2 and $\mu > 0$. A detailed description of the generated points is given in Table I. The major background for the like sign dimuon signature comes from multijet background from QCD processes, mostly $b\bar{b}$, and has been estimated from data. More details on the multijet background estimation are provided in section III. The other main background sources come from WZ, ZZ, $Z/\gamma^* + jet(s)$ and $W + jet(s)$ processes with subsequent decays into muons.

TABLE I: Values of m_0 and $m_{1/2}$ parameters for the generated points. The other parameters are set to the following values: $\tan\beta = 3$, $A_0 = 0$ GeV/c^2 and $\mu > 0$. The masses of $\widetilde{\chi}_2^0$, $\widetilde{\chi}_1^{\pm}$, $\widetilde{\ell}_R$, $\widetilde{\tau}_1$ and the NLO cross-section from reference [10] times branching fraction into three leptons are also indicated.

point	$\boldsymbol{m_0}$	$\boldsymbol{m_{1/2}}$	$\boldsymbol{m_{\widetilde{\chi}_2^0}}$	$\boldsymbol{m_{\widetilde{\chi}_1^{\pm}}}$	$\boldsymbol{m_{\widetilde{\ell}_R}}$	$\boldsymbol{m_{\widetilde{\tau}_1}}$	$\boldsymbol{\sigma_{\rm NLO} \times BR(3\ell)}$
	GeV/c^2	GeV/c^2	GeV/c^2	GeV/c^2	GeV/c^2	GeV/c^2	fb
B2	68	170	108.2	104.3	100.6	99.2	838±7
C2	72	175	112.4	108.9	104.4	103.1	713±6
D2	76	180	116.7	113.3	108.4	107.0	596±4
E2	80	185	120.9	117.7	112.3	111.0	511±4
F2	98	205	138.0	135.6	129.8	128.7	180±3

III. EVENT SELECTION

Selected events are required to pass a set of dimuon triggers with a p_T threshold close to 5 GeV/c and to have two like sign muons matched to central tracks with $p_T > 5$ GeV/c. The background is dominated by muons from b-decays which are less isolated than muons from signal. In the following, the muon isolation is defined by the activity near the muon candidate in the calorimeter and/or tracker. Two muon isolation criteria are considered.

muon tightly isolated:

- $E_T^{0.1<\Delta R<0.4} < 2.5$ GeV
- $p_T^{\Delta R<0.5} < 2.5$ GeV/c

muon loosely isolated:

- $E_T^{0.1<\Delta R<0.4} < 4$ GeV
- $p_T^{\Delta R<0.5} < 4$ GeV/c

where $E_T^{0.1<\Delta R<0.4}$ stands for the sum of the energy depositions in all the calorimeter cells lying in a calorimeter hollow cone with inner and outer radii respectively set to $R_{inner} = 0.1$ and $R_{outer} = 0.4$ and $p_T^{\Delta R<0.5}$ stands for the transverse momentum sum of all the tracks (excluding the muon candidate) lying in a tracker cone with radius $R = 0.5$. All cones are centered around the muon candidate direction. The variable ΔR is defined as $\Delta R = \sqrt{\Delta\eta^2 + \Delta\varphi^2}$ with $\Delta\eta$ and $\Delta\varphi$ respectively the distance in pseudo-rapidity and the angular difference in

the plane transverse to the beam direction. One muon is required tightly isolated and the second one loosely isolated. Both muons are required to be no further than 1 cm from the primary vertex measured along the beam direction.

The multijet background, mostly muons from b-decays, has been estimated from the data as follows. Muons coming from the signal tend to be more isolated than those from multijet background processes. The sample used is formed with the data events which fullfill the previous requirements except isolation criterion and is divided in two subsamples:

i) with one tightly isolated muon and one loosely isolated muon (sample $\mathcal{S}$),

ii) with one tightly isolated muon and one muon failing the loose isolation criterion (sample $\mathcal{Q}$).

Then, to estimate the number of events coming from multijet background processes, the sample $\mathcal{Q}$ has been normalized to the sample $\mathcal{S}$. To avoid any bias, the normalization has been performed in the region $\Delta\varphi(\mu,\mu) \geq 2.9$, dominated by $b\bar{b}$ events. The normalization factor of the transverse momentum distribution of the non isolated muon from sample $\mathcal{Q}$ and the muons from sample $\mathcal{S}$ is defined as

$$R(p_T) = \frac{1}{2}\frac{\mathcal{S}(p_T)}{\mathcal{Q}(p_T^{not\ isolated})}\bigg|_{\Delta\varphi(\mu,\mu)\geq 2.9}$$

The multijet background sample corresponds to the events in the sample $\mathcal{Q}$ with $\Delta\varphi(\mu,\mu) < 2.9$ weighted with $R(p_T)$ according to the transverse momentum of the non isolated muon.

Due to the multijet background estimation procedure, a cut $\Delta\varphi(\mu,\mu) < 2.9$ is added. All the previously listed cuts are referred as the selection $\mathcal{A}$. Several additional cuts are studied in order to extract the signal from the background.

Missing transverse energy:

The $\widetilde{\chi}_1^0$ produced in $\widetilde{\chi}_1^\pm$ and $\widetilde{\chi}_2^0$ decays is stable and escapes detection leading to a significant amount of missing transverse energy. For events with jets with transverse energies above 15 GeV, a cut on the significance, Sig($\not\!\!E_T$), is used. The Sig($\not\!\!E_T$) is defined by normalizing the $\not\!\!E_T$ to σ_{proj}, a measure of the jet energy resolution projected onto the $\not\!\!E_T$ direction:

$$\mathrm{Sig}(\not\!\!E_T) = \frac{\not\!\!E_T}{\sqrt{\sum_{\mathrm{jets}} \sigma^2_{proj}}}$$

The distributions of both missing transverse energy and Sig($\not\!\!E_T$) for data, signal and background processes are presented in Figure 4.

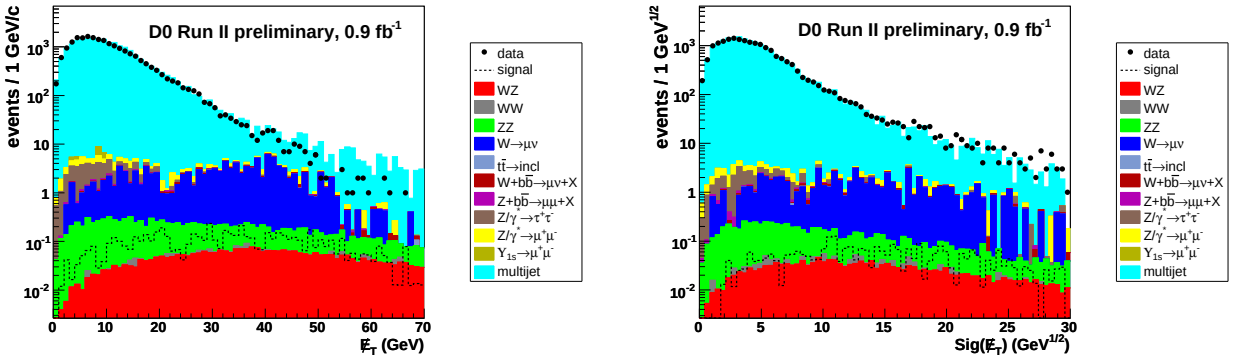

FIG. 4: Distributions of the missing transverse energy (left) and Sig($\not\!\!E_T$) (right) observed in data and expected for the background and signal. The selection $\mathcal{A}$ is applied.

Invariant masses:

Cuts on the invariant masses of opposite sign and like sign dimuon pairs have been studied in order to reduce respectively the contribution of background events with a Z boson decaying into two opposite sign muons and multijet background which is expected in the low mass region. A cut on the transverse mass computed using the missing transverse energy and the next to leading muon p_T is also used to reject events from diboson and W background processes. The distributions of these variables are displayed in Figure 5.

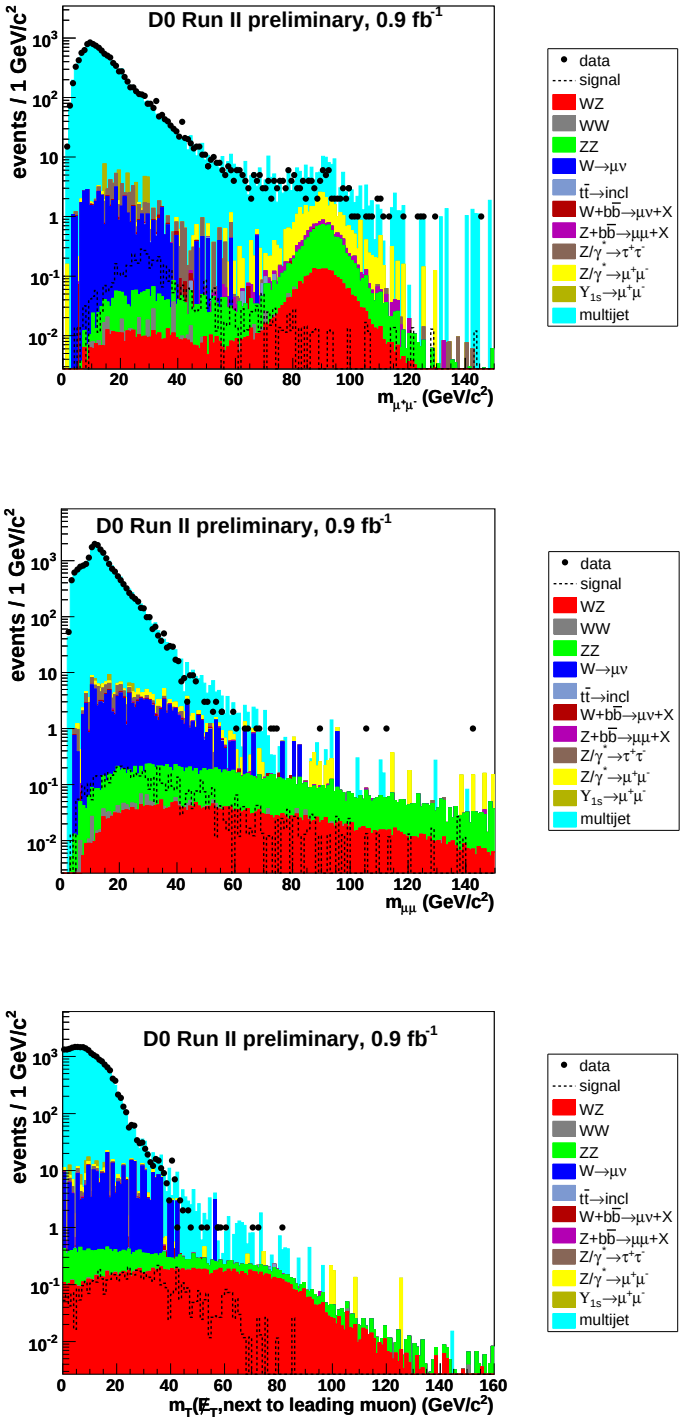

FIG. 5: Distributions of the invariant masses of opposite sign (top) and like sign (middle) muon pairs and of the transverse mass computed using the missing transverse energy and the next to leading muon p_T (bottom) observed in data and expected for the background and signal. The selection $\mathcal{A}$ is applied.

Momenta:

Cuts on the muon momenta have been optimized to reject the multijet background. The distributions of the transverse momentum for the leading and next to leading muons and the distribution of the missing transverse energy times the next to leading muon p_T are presented in Figure 6.

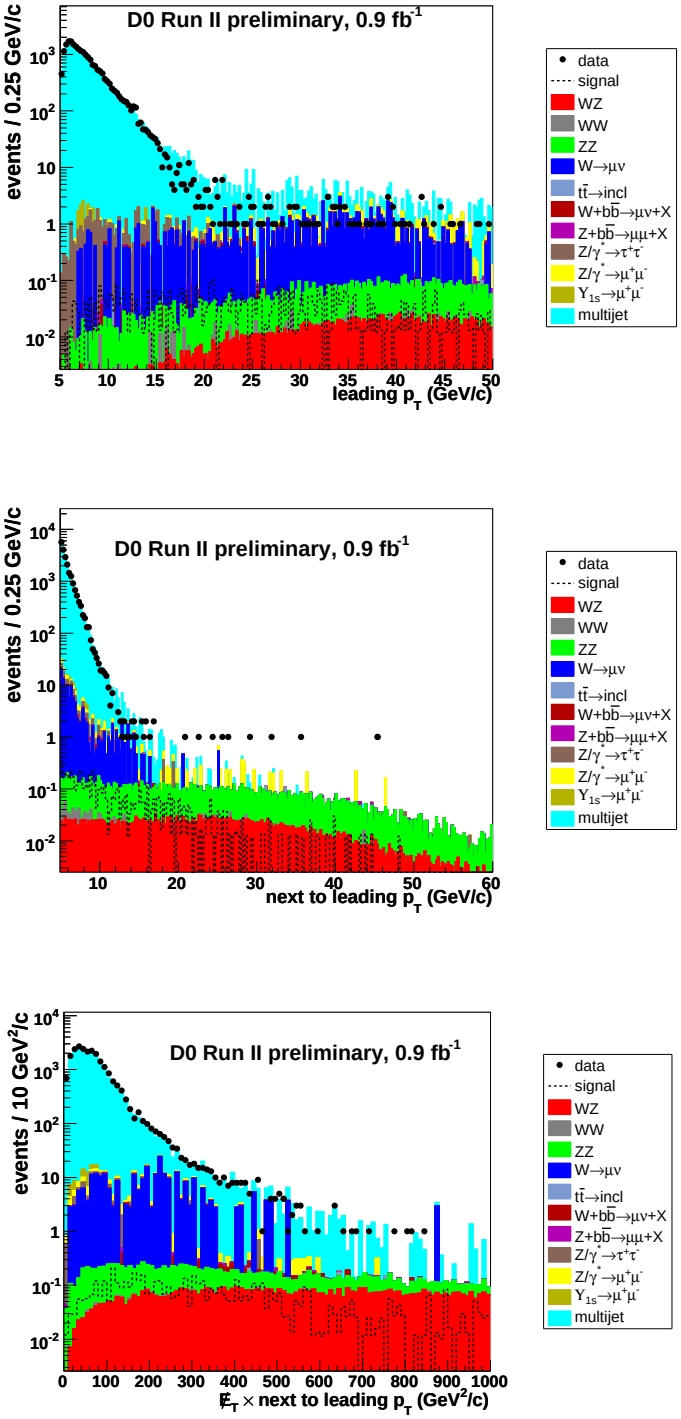

FIG. 6: Distributions of the transverse momentum for the leading (top) and next to leading (middle) muons and of the missing transverse energy times the next to leading muon p_T (bottom) observed in data and expected for the background and signal. The selection $\mathcal{A}$ is applied.

Those criteria have been optimized to get the best expected limit on the quantity $\sigma(p\bar{p} \to \widetilde{\chi}_1^{\pm}\widetilde{\chi}_2^0) \times BR(3\ell)$ using the modified frequentist approach defined in the reference [11] with a special emphasis on topologies with a very soft third lepton. The point C2 ($m_0 = 72$ GeV/c^2, $m_{1/2} = 175$ GeV/c^2, $\tan\beta = 3$, $A_0 = 0$ GeV/c^2 and $\mu > 0$) has been used to perform the optimization and the results are summarized in Table II.

TABLE II: Summary of selection criteria obtained after optimization.

a	$M_{\mu^\pm\mu^\mp} \in [25-65]$ GeV/c^2 if opposite sign pairs are reconstructed
b	$p_T^{\mu^2} < 35$ GeV/c
c	$p_T^{\mu^2} > 8$ GeV/c
d	$p_T^{\mu^1} > 13$ GeV/c
e	$M_{\mu^\pm\mu^\pm} \in [12-110]$ GeV/c^2
f	$M_T(\not\!\!E_T, p_T^{\mu^2}) \in [15-65]$ GeV/c^2
g	$\not\!\!E_T > 10$ GeV
h	$\mathrm{Sig}(\not\!\!E_T) > 12$ GeV$^{1/2}$
i	$\not\!\!E_T \times p_T^{\mu^2} > 160$ GeV^2/c

IV. RESULTS

The number of events expected for background processes and observed in data after each step of the selection is listed in Table III. The single event observed in data is consistent with the 1.1±0.4 events expected from background.

TABLE III: Number of events expected from background processes and observed in data at the different levels of the selection.

cut	**QCD**	**WZ**	**ZZ**	$\boldsymbol{W \to \mu\nu}$	$\boldsymbol{Z/\gamma^* \to \mu^+\mu^-}$	$\boldsymbol{Z/\gamma^* \to \tau^+\tau^-}$
selection $\mathcal{B}$	14787±981	3.3±0.2	9.7±0.7	58±7	42±5	6.5±1.4
$M_{\mu^\pm\mu^\mp} \in [25-65]$ GeV/c^2 (a)	3452±232	0.66±0.05	0.70±0.06	16±3	4.2±1.0	1.7±0.4
$p_T^{\mu^2} < 35$ GeV/c (b)	3452±232	0.53±0.04	0.64±0.06	16±3	4.2±1.0	1.7±0.4
$p_T^{\mu^2} > 8$ GeV/c (c)	4.9±1.5	0.42±0.03	0.43±0.04	1.9±0.9	0.4±0.2	0.29±0.14
$p_T^{\mu^1} > 13$ GeV/c (d)	2.8±1.1	0.41±0.03	0.42±0.04	1.9±0.9	0.4±0.2	0.11±0.11
$M_{\mu^\pm\mu^\pm} \in [12-110]$ GeV/c^2 (e)	1.4±0.7	0.39±0.03	0.38±0.04	1.9±0.9	0.4±0.2	0.11±0.11
$M_T(\not\!\!E_T, p_T^{\mu^2}) \in [15-65]$ GeV/c^2 (f)	0.9±0.5	0.32±0.02	0.32±0.04	0.7±0.5	0.4±0.2	0
$\not\!\!E_T > 10$ GeV (g)	0.5±0.3	0.30±0.02	0.27±0.03	0.7±0.5	0.3±0.2	0
$\mathrm{Sig}(\not\!\!E_T) > 12$ GeV$^{1/2}$ (h)	0.19±0.19	0.198±0.015	0.16±0.02	0.7±0.5	0.21±0.14	0
$\not\!\!E_T \times p_T^{\mu^2} > 160$ GeV^2/c (i)	0.19±0.19	0.194±0.015	0.16±0.02	0.2±0.2	0.21±0.14	0

	$\boldsymbol{W b\bar{b}}$	$\boldsymbol{Z b\bar{b}}$	**WW**	$\boldsymbol{\Upsilon_{1s}}$	$\boldsymbol{t\bar{t}}$	**sum**	**data**
selection $\mathcal{B}$	3.2±0.3	2.5±0.2	0.14±0.02	8.4±3.5	1.3±0.4	14922±981	15234
$M_{\mu^\pm\mu^\mp} \in [25-65]$ GeV/c^2 (a)	0.37±0.06	2.3±0.3	0.13±0.03	0.6±0.3	0.8±0.3	3479±232	3569
$p_T^{\mu^2} < 35$ GeV/c (b)	0.35±0.06	2.3±0.3	0.13±0.03	0.6±0.3	0.55±0.17	3479±232	3358
$p_T^{\mu^2} > 8$ GeV/c (c)	0.09±0.03	0.21±0.07	0.026±0.009	0	0.23±0.07	8.9±1.8	10
$p_T^{\mu^1} > 13$ GeV/c (d)	0.08±0.03	0.21±0.07	0.026±0.009	0	0.15±0.05	6.5±1.4	6
$M_{\mu^\pm\mu^\pm} \in [12-110]$ GeV/c^2 (e)	0.07±0.02	0.21±0.07	0.023±0.009	0	0	4.9±1.2	2
$M_T(\not\!\!E_T, p_T^{\mu^2}) \in [15-65]$ GeV/c^2 (f)	0.06±0.02	0.19±0.07	0.013±0.006	0	0	2.9±0.8	2
$\not\!\!E_T > 10$ GeV (g)	0.05±0.02	0.19±0.07	0.006±0.003	0	0	2.3±0.7	1
$\mathrm{Sig}(\not\!\!E_T) > 12$ GeV$^{1/2}$ (h)	0.03±0.015	0.16±0.06	0.006±0.003	0	0	1.7±0.6	1
$\not\!\!E_T \times p_T^{\mu^2} > 160$ GeV^2/c (i)	0.02±0.014	0.16±0.06	0.006±0.003	0	0	1.1±0.4	1

The number of expected events and the efficiencies for the signal at different levels of cuts are presented in Table IV.

TABLE IV: Number of events (top) and efficiencies in % (bottom) expected from signal after each step of the selection. Sets of mSUGRA parameters defined in Table I are under consideration.

cut	**B2**	**C2**	**D2**	**E2**	**F2**
preselection ($\mathcal{A}$)	8.4±0.6	7.4±0.6	6.2±0.5	5.6±0.4	3.0±0.2
$M_{\mu^\pm\mu^\mp} \in [25-65]$ GeV/c^2 (a)	7.9±0.6	6.9±0.5	5.7±0.4	5.3±0.4	2.7±0.2
$p_T^{\mu^2} < 35$ GeV/c (b)	7.6±0.6	6.6±0.5	5.4±0.4	5.2±0.4	2.49±0.19
$p_T^{\mu^2} > 8$ GeV/c (c)	6.4±0.5	5.8±0.5	4.7±0.4	4.9±0.4	2.12±0.14
$p_T^{\mu^1} > 13$ GeV/c (d)	5.8±0.5	5.2±0.4	4.2±0.3	4.2±0.3	2.00±0.16
$M_{\mu^\pm\mu^\pm} \in [12-110]$ GeV/c^2 (e)	5.7±0.5	5.2±0.4	4.2±0.3	4.2±0.3	2.00±0.16
$M_T(\not\!\!E_T, p_T^{\mu^2}) \in [15-65]$ GeV/c^2 (f)	5.4±0.4	5.0±0.4	4.0±0.3	3.8±0.3	1.90±0.13
$\not\!\!E_T > 10$ GeV (g)	4.8±0.4	4.7±0.4	3.6±0.3	2.9±0.2	1.59±0.13
Sig($\not\!\!E_T$) > 12 GeV$^{1/2}$ (h)	4.6±0.4	4.4±0.3	3.4±0.3	2.6±0.2	1.51±0.13
$\not\!\!E_T \times p_T^{\mu^2} > 160$ GeV^2/c (i)	4.0±0.4	4.0±0.3	2.9±0.3	2.4±0.2	1.33±0.12

cut	**B2**	**C2**	**D2**	**E2**	**F2**
preselection ($\mathcal{A}$)	26.0±1.0	27.5±1.0	28.2±1.0	26.7±1.0	30.4±1.1
$M_{\mu^\pm\mu^\mp} \in [25-70]$ GeV/c^2 (a)	24.5±1.0	25.6±1.0	25.8±1.0	25.4±0.9	27.5±1.0
$p_T^{\mu^2} < 35$ GeV/c (b)	23.5±0.9	24.5±1.0	24.8±1.0	24.7±0.9	25.3±1.0
$p_T^{\mu^2} > 8$ GeV/c (c)	20.0±0.9	21.3±0.9	21.3±0.9	23.4±0.9	21.6±0.9
$p_T^{\mu^1} > 13$ GeV/c (d)	18.0±0.9	19.3±0.9	19.2±0.9	20.3±0.9	20.4±0.9
$M_{\mu^\pm\mu^\pm} \in [12-110]$ GeV/c^2 (e)	17.8±0.8	19.1±0.9	19.1±0.9	20.3±0.9	20.4±0.9
$M_T(\not\!\!E_T, p_T^{\mu^2}) \in [15-65]$ GeV/c^2 (f)	16.7±0.8	18.4±0.8	18.2±0.9	17.9±0.8	19.4±0.9
$\not\!\!E_T > 10$ GeV (g)	15.0±0.8	17.5±0.8	16.5±0.8	13.8±0.7	16.3±0.9
Sig($\not\!\!E_T$) > 12 GeV$^{1/2}$ (h)	14.4±0.8	16.5±0.8	15.5±0.8	12.3±0.7	15.6±0.8
$\not\!\!E_T \times p_T^{\mu^2} > 160$ GeV^2/c (i)	12.5±0.7	14.8±0.8	13.4±0.8	11.5±0.7	13.7±0.8

The estimates for expected numbers of background and signal events depend on numerous measurements that each introduce a systematic uncertainty: integrated luminosity (6.5%), trigger efficiencies (1–2%), lepton identification and reconstruction efficiencies (1–2%), jet energy scale calibration in signal ($< 4\%$) and background events (7–20%), lepton momentum calibration (1%), detector modeling (2%), PDF uncertainties ($< 4\%$), and modeling of multijet background (4–40%).

A limit on the quantity $\sigma(p\bar{p} \to \widetilde{\chi}_1^\pm \widetilde{\chi}_2^0) \times BR(3\ell)$ has been derived under the assumption $m_{\widetilde{\ell}_R} \lesssim m_{\widetilde{\chi}_2^0}$ (so called points B2, C2, D2, E2 and F2) where the like sign dimuon selection plays a major role due to the softness of the third lepton. Observed and expected limits considering those points are presented in Figure 7 as a function of $\widetilde{\chi}_1^\pm$ mass. The region above the curve is excluded at 95% CL using the modified frequentist approach defined in the reference [11].

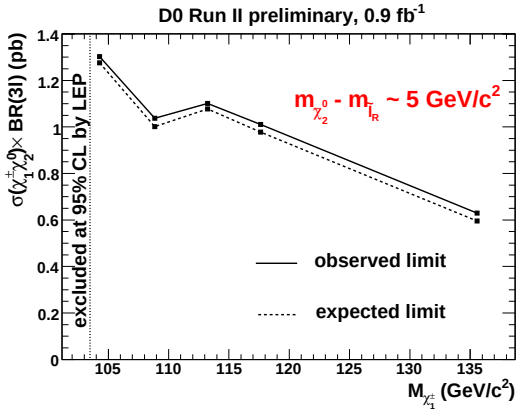

FIG. 7: Limits on $\sigma(p\bar{p} \to \widetilde{\chi}_1^\pm \widetilde{\chi}_2^0) \times BR(3\ell)$ for $m_{\widetilde{\ell}_R} \lesssim m_{\widetilde{\chi}_2^0}$ mSUGRA points. The $\widetilde{\chi}_1^\pm$ mass region below 103.5 GeV/c^2 is excluded by LEP search [9]. The region above the curve is excluded at 95% CL. The squares correspond to the five mSUGRA points defined in Table I.

The result of this analysis is combined with the results of $\mu\mu\ell$ and $e\mu\ell$ from reference [5] and a newly updated $ee\ell$ analysis [12] using the modified frequentist approach. The points under consideration for the combination as well as the number of expected events and the signal efficiency after the like sign dimuon selection has been applied are presented in Table V. Those points, without slepton mixing and with sleptons slightly heavier than $\widetilde{\chi}_1^{\pm}$ and $\widetilde{\chi}_2^0$, correspond to the 3ℓ-max scenario which lead to an enhanced leptonic branching fraction.

TABLE V: Values of m_0 and $m_{1/2}$ parameters for the points used in combination. The other parameters are set to the following values: $\tan\beta = 3$, $A_0 = 0$ GeV/c^2 and $\mu > 0$. The masses of $\widetilde{\chi}_2^0$, $\widetilde{\chi}_1^{\pm}$, $\widetilde{\ell}_R$, the cross-section times branching fraction into three leptons, the number of expected events and the signal efficiency once the like sign dimuon selection has been applied are also indicated.

point	m_0 GeV/c^2	$m_{1/2}$ GeV/c^2	$m_{\widetilde{\chi}_2^0}$ GeV/c^2	$m_{\widetilde{\chi}_1^{\pm}}$ GeV/c^2	$m_{\widetilde{\ell}_R}$ GeV/c^2	$\sigma \times BR(3\ell)$ pb	$\mathbf{N_{expected}}$	**efficiency** %
SLHA.244.324	121	221	152	150	153	0.058	0.61±0.02	11.9±0.5
SLHA.131.232	98	192	127	125	129	0.14	2.24±0.09	12.6±0.5
SLHA.87.194	88	182	118	115	119	0.22	3.76±0.15	13.6±0.6

The fraction of signal events that is selected by more than one selection is assigned to the selection with the largest signal-to-background ratio and removed from all others. The expected and observed limits are shown in Figure 8 as a function of the $\widetilde{\chi}_1^{\pm}$ mass. This result improves significantly the upper limit of about 0.2 pb set by reference [5]. The cross-section limit set corresponds to a $\widetilde{\chi}_1^{\pm}$ mass limit of 140 GeV/c^2 in the 3ℓ-max scenario.

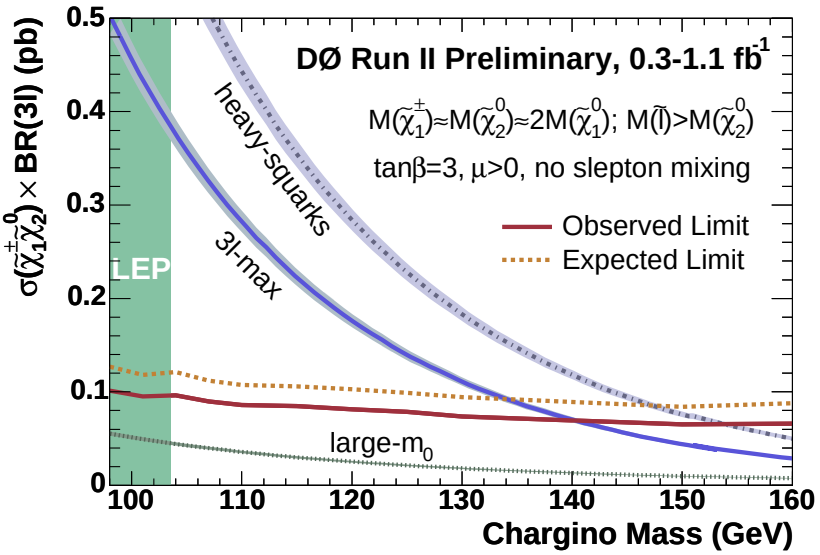

FIG. 8: Limits on $\sigma \times BR(3\ell)$ as a function of $\widetilde{\chi}_1^{\pm}$ mass, in comparison with the expectation for several mSUGRA scenarios. PDF and renormalization/factorization scale uncertainties are shown as shaded bands. A limit of 140 GeV/c^2 on the $\widetilde{\chi}_1^{\pm}$ mass has been set considering a mSUGRA scenario with sleptons slightly heavier than $\widetilde{\chi}_1^{\pm}$ and no slepton mixing. This limit is extracted from reference [12].

V. CONCLUSION

A search for the associated production of $\widetilde{\chi}_1^{\pm}$ and $\widetilde{\chi}_2^0$ in the like sign dimuon channel using a dataset corresponding to an integrated luminosity of 0.9 fb^{-1} has been performed. The selection has been optimized in order to obtain the best expected limit on the quantity $\sigma(p\bar{p} \to \widetilde{\chi}_1^{\pm}\widetilde{\chi}_2^0) \times BR(3\ell)$. The observation of one event in the data is consistent with the 1.1±0.4 events expected from the background. A limit, which improves previous results has been set. For mSUGRA scenarios with enhanced leptonic branching fractions, a $\widetilde{\chi}_1^{\pm}$ mass limit beyond the reach of LEP searches has been set.

Acknowledgement

We thank the staffs at Fermilab and collaborating institutions, and acknowledge support from the DOE and NSF (USA);CEA and CNRS/IN2P3 (France);FASI, Rosatom and RFBR (Russia);CAPES, CNPq, FAPERJ, FAPESP and FUNDUNESP (Brazil);DAE and DST (India);Colciencias (Colombia);CONACyT (Mexico);KRF and KOSEF (Korea);CONICET and UBACyT (Argentina);FOM (The Netherlands);PPARC (United Kingdom);MSMT (Czech Republic);CRC Program, CFI, NSERC and WestGrid Project (Canada);BMBF and DFG (Germany);SFI (Ireland);The Swedish Research Council (Sweden);Research Corporation;Alexander von Humboldt Foundation;and the Marie Curie Program.

---

[1] H. Nilles, *Supersymmetry supergravity and particle physics*, Phys. Rep. **110** (1984) 1; H. Haber et G. Kane, *The search for supersymmetry: probing physics beyond the standard model*, Phys. Rep. **117** (1985) 75.

[2] S. Dawson, *The MSSM and why it works*, BNL-HET-SD-97-4 (1997), hep-ph/9712464.

[3] E. Cremmer *et al.*, *Superhiggs effect in supergravity with general scalar interactions*, Phys. Lett. **B79** (1978) 231; E. Cremmer *et al.*, *Spontaneous symmetry breaking and Higgs effect in supergravity without cosmologocal constant*, Nucl. Phys. **B147** (1979) 105.

[4] P. Fayet, *Spontaneously broken supersymmetric theories of weak, electromagnetic and strong interactions*, Phys. Lett. **B69** (1977) 489; P. Fayet, *Mixing between gravitational and weak interactions through the massive gravitino*, Phys. Lett. **B70** (1977) 461; G. Farrar and P. Fayet, *Phenomenology of the production, decay and detection of new hadronic states associated with supersymmetry*, Phys. Lett. **B76** (1978) 575.

[5] DØ Collaboration, *Search for supersymmetry via associated production of charginos and neutralinos in final states with three leptons*, Fermilab-Pub-05-075-E, Phys. Rev. Lett. **95** 151805 (2005), hep-ex/0504032.

[6] T. Sjöstrand, Comp. Phys. Commun. **82** (1994) 74.

[7] W. Porod, Comp. Phys. Commun. **153** (2003) 275.

[8] P. Skands,*SUSY Les Houches Accords: interfacing SUSY spectrum calculators, decay packages and event generators* , JHEP **0407** (2004) 036.

[9] LEPSUSYWG, ALEPH, DELPHI, L3 and OPAL experiments, *Charginos, large* m_0 LEPSUSYWG/01-03.1 (lepsusy.web.cern.ch/lepsusy/Welcome.html).

[10] W. Beenakker *et al.*, *The production of charginos/neutralinos and sleptons at hadron colliders*, Phys. Rev. Lett. **83** (1999) 3780, hep-ph/9906298.

[11] T. Junk, *Confidence level computation for combining searches with small statistics*, Nucl. Instrum. Meth. **A434** (1999) 435.

[12] DØ Collaboration, *Search for the associated production of chargino and neutralino in final states with two electrons and an additional lepton*, DØ note 5127.